See discussions, stats, and author profiles for this publication at: https://www.researchgate.net/publication/264935404

Dopamine Adsorption on TiO2 Anatase Surfaces

ARTICLE in THE JOURNAL OF PHYSICAL CHEMISTRY C · AUGUST 2014

Impact Factor: 4.77 · DOI: 10.1021/jp506156e

CITATION	READS
1	62

7 AUTHORS, INCLUDING:



Arne Keller

Université Paris-Sud 11

71 PUBLICATIONS 1,181 CITATIONS

SEE PROFILE



Tarakeshwar Pilarisetty

Arizona State University

99 PUBLICATIONS 4,699 CITATIONS

SEE PROFILE



Vladimiro Mujica

Arizona State University

140 PUBLICATIONS 3,135 CITATIONS

SEE PROFILE

Article

pubs.acs.org/JPCC

Dopamine Adsorption on TiO₂ Anatase Surfaces

- $_2$ I. Urdaneta, $^{\dagger, \ddagger, \$}$ A. Keller, $^{\$}$ O. Atabek, $^{\$}$ J. L. Palma, $^{\parallel}$ D. Finkelstein-Shapiro, $^{\parallel}$ T. Pilarisetty, $^{\parallel}$ V. Mujica, $^{\parallel}$ and M. Calatayud*, $^{\dagger, \ddagger, \bot}$
- 4 [†]UMR 7616, Laboratoire de Chimie Théorique, Sorbonne Universités, UPMC Univ. Paris 06, F-75005 Paris, France
- 5 [‡]CNRS, UMR 7616, Laboratoire de Chimie Théorique, Université P. M. Curie, P.O. Box 137 F-75005, F-75005, Paris, France
- 6 §Institut des Sciences Moléculaires d'Orsay (ISMO) Bât 350, UMR8214 CNRS-Université Paris-Sud, Orsay, France
- ⁷ Department of Chemistry and Biochemistry, Arizona State University, P.O. Box 871604, Tempe, Arizona 85287, United States
- 8 ¹Institut Universitaire de France, France
- 9 Supporting Information

10

11

12

13

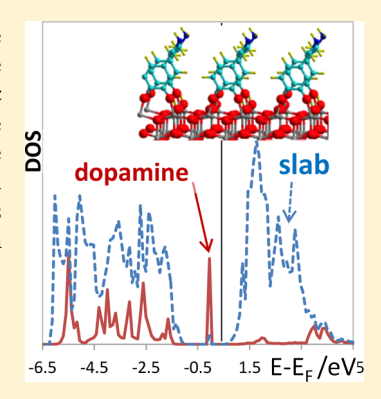
14

1.5

16

17

ABSTRACT: The dopamine-TiO₂ system shows a specific spectroscopic response, surface enhanced Raman scattering (SERS), whose mechanism is still unknown. In this study, the goal is to reveal the key role of the molecule—nanoparticle interface in the electronic structure by means of *ab initio* modeling. The dopamine adsorption energy on anatase surfaces is computed and related to changes in the electronic structure. Two features are observed: the appearance of a state in the material band gap, and charge transfer between molecule and surface upon electronic excitation. The analysis of the energetics of the systems would point to a selective adsorption of dopamine on the (001) and (100) terminations, with much less affinity for the (101) plane.



19 INTRODUCTION

20 In the past decade, much effort has been devoted to the study 21 of TiO₂ nanoclusters because of their multiple applications in 22 chemistry. Considerable attention has been given to the 23 adsorption of organic molecules on TiO2 clusters since these 24 systems have shown specific optical properties in dye-sensing or 25 photocatalysis.² Very recently, an important increase of the 26 emitted Raman signal has been observed upon adsorption of 27 dopamine on titania nanoparticles (NP) with respect to the 28 bare molecule.³⁻⁹ This phenomenon, known as surface 29 enhanced Raman scattering (SERS), is quite common for 30 metallic supports but is much less characterized for semi-31 conducting materials. The mechanism explaining the enhance-32 ment of the Raman signal in the dopamine-TiO2 system has 33 been postulated to be one-electron charge transfer, 10,11 from 34 the molecule to the nanoparticle. The goal of the present article 35 is to investigate the interface dopamine-TiO2 on an atomic level 36 by means of density functional theory (DFT) periodic 37 boundary condition calculations in order to elucidate the 38 features connecting geometrical and electronic structures. It will 39 be shown that the electronic structure of the surface of the 40 complex system dopamine-anatase is essential to explain the 41 basic features of the observed SERS.

SERS was observed on a series of experiments^{3,4} for annoparticles between 2 to 5 nm diameter at different dopamine contents, in chloride acid solution at pH 4 for laser excitation wavelengths going from 500 to 800 nm. The adsorption site and strength play a key role in the SERS effect.

Experimentally, it is known that dopamine adsorbs perpendic- 47 ular to the TiO2 surface of the nanoparticle through its oxygen 48 atom, which is bonded to a surface Ti site.³ However, it is yet 49 unclear if it is a monodentate adsorption (only one dopamine 50 oxygen is linked to one Ti), bidentate adsorption (both oxygen 51 sites are linked to adjacent Ti atoms), or chelated adsorption 52 (both oxygen sites are adsorbed on the same Ti). NEXAFS 53 experiments on isolated dopamine and dopamine on anatase 54 TiO₂ (101)¹² and rutile (110)¹³ showed that the molecule 55 interacts strongly with the surface, in agreement with 56 theoretical calculations. Previous studies on catechol interaction 57 with TiO₂ nanoparticles, a hybrid of great importance for solar 58 technologies whose geometry is close to dopamine, pointed out 59 the crucial role of the adsorption mode of the molecule on the 60 optical properties. 14-17 The experimental and theoretical 61 literature on catechol conclude that dissociative adsorption of 62 the molecule in bidentate mode on the rutile (110) anatase 63 (101) surfaces occurs, 13 with easy interconversion to 64 monodentate upon reprotonation. 18 Chelated geometries are 65 found to be stable in the presence of defective TiO₂, 15 although 66 their electronic structure might not result in the formation of a 67 band gap state.¹⁹ In the present article, we focus on the 68 adsorption systems of neutral dopamine on a series of anatase 69

Received: June 20, 2014 Revised: July 31, 2014 70 surfaces in order to unravel structural and electronic features to 71 explain the observed SERS.

Modeling hybrid systems has been undertaken in the past by 73 considering small TiO_2 nanoclusters $(TiO_2)_N$ N = 2,4,...10 and 74 one dopamine molecule. These investigations indicate that 75 the dopamine effect on the TiO₂ cluster electronic structure is 76 2-fold: first, it gives rise to new occupied states (coming mainly 77 from the molecule) inside the cluster's original band gap, and 78 second, it gives rise to a large charge polarization effect 79 involving the HOMO-LUMO orbitals of the complex since 80 the HOMO is localized mainly in the molecule, while the 81 LUMO is mostly localized in the nanocluster. The use of small 82 nanoclusters as models for hybrid systems allows one to 83 consider quantum confinement, which is one of the main 84 reasons for the onset of size-dependent properties in these 85 systems.²⁰ However, such models might not be directly 86 comparable to the real systems because (i) their size is really 87 small, a few angstroms, whereas the real nanoparticles are few 88 nanometers diameter, (ii) the concentration of dopamine 89 modeled is high, and (iii) there are many low coordinated 90 atoms in the cluster, much more than in real surfaces, like 91 titanyl Ti=O, 3- or 4-fold titanium sites. In the present work, 92 we use periodic slabs to investigate the geometrical, energetic, 93 and electronic features of dopamine on bare anatase surfaces, 94 focusing on molecule-surface behavior that occurs on the 95 atomic level. In such a model, the excited states form a 96 conduction band instead of discrete states arising from the use 97 of cluster models and therefore bring important complementary 98 information on the electronic structure of dopamine-NP hybrid 99 systems. To the best of our knowledge, the use of slab models 100 for the dopamine-anatase system has not been reported yet.

In the present article, the dopamine adsorption on three 102 different anatase terminations is investigated so as to character-103 ize the effect of the surface topology in the interaction between 104 the molecule and the semiconducting nanoparticle. It will be 105 shown that for the three slabs investigated dopamine 106 chemisorbs following a double deprotonation and forming 107 two O-Ti bonds with two surface Ti sites. However, the 108 dopamine-titania interaction is energetically more favorable for 109 (001) and (100) terminations than for (101) indicating a 110 possible selectivity in the adsorption. The electronic structure 111 of the most stable models shows a molecular state located in 112 the slab TiO₂ band gap whose position depends on the surface 113 termination. Moreover, the excitation to a triplet state shows 114 the interaction of the HOMO located in the molecule and the 115 LUMO located in the surface Ti sites. The electronic structure 116 obtained for dopamine adsorbed on anatase slabs is therefore 117 consistent with the charge transfer associated with the SERS 118

The article is organized as follows. First, the methods and models used are described. Second, the adsorption modes of dopamine on selected anatase surfaces are presented. Third, the electronic structure of ground and excited states of selected systems is analyzed. A section of conclusions closes the article.

METHODS AND MODELS

125 Calculations are performed using the VASP 5.3.3 code 25,26 with 126 the Perdew–Becke–Ernzerhof functional. The core electrons 127 are kept frozen by the plane augmented wave method 128 PAW. The valence electrons (Ti, 4s² 3d²; O, 2s² 2p⁴; C, 129 2s² 2p²; N, 2s² 2p⁵; H, 1s¹) are explicitly described by means of 130 a plane-wave basis set with a cutoff at 400 eV. A vacuum of at 131 least 20 Å in the c direction, orthogonal to the slab, is kept in

order to prevent interaction between successive slabs, repeated 132 in three dimensions. The reciprocal space was sampled with a 133 Monkhorst–Pack grid adapted to the dimensions of each 134 system, the distance between two k-points in the reciprocal 135 space being $\sim 0.05 \text{ Å}^{-1}$. Geometrical optimization is carried out 136 by means of the conjugate-gradient algorithm with a tolerance 137 of $^{0.1}$ meV in total energy; all atoms are allowed to relax. 138 Dipole corrections have been included in the direction 139 perpendicular to the slab.

In order to give a description of the electronic structures, the 141 singlet closed-shell optimized geometry has been chosen as the 142 starting point. From this structure, a single-point calculation 143 with $3 \times 3 \times 1$ k-point sampling is done to calculate the 144 corresponding density of states (DOS). Then, the excited states 145 are simulated by an excitation of the structure to a triplet $(N_{\alpha-\beta})$ 146 = 2) state. This approach allows giving an estimate of the 147 relative energy of the electronic states, as well as the 148 contributions of both molecule and slab to the DOS. An 149 analysis of the electron spin density is done to get a picture of 150 the charge transfer occurring upon dopamine adsorption on 151 anatase TiO2. Since the pure GGA functional gives an artificial 152 delocalization of the electron in the triplet excited state, we 153 have conducted these calculations at the GGA+U level, i.e., a 154 Hubbard parameter U-I = 4 has been included for Ti 3d orbitals 155 to account for the self-interaction error.

As models, three planes of the anatase phase have been 157 considered: (101), (001), and (100), on top of which one 158 dopamine molecule is adsorbed in different configurations. The 159 unit cells have been chosen so as to allow a reasonable coverage 160 of 0.25 molecules per surface titanium sites. Table 1 shows the 161 th

Table 1. Geometrical Parameters of the Slab Models and Calculated Adsorption Energy for Dopamine Adsorption^a

	(001)	(100)	(101)
unit cell	2×2	2×1	2×2
a (Å)	7.57	7.57	7.57
b (Å)	7.57	9.51	10.91
c (Å)	40	40	40
slab thickness (Å)	13.4	13.8	13.1
composition	$\mathrm{Ti}_{24}\mathrm{O}_{48}$	$\mathrm{Ti_{32}O_{64}}$	$\mathrm{Ti_{32}O_{64}}$
$E_{ m ads}$ in eV	-1.86	-1.14	-0.67

^aEach slab model has 4 surface titanium atoms.

dimensions of the unit cells chosen. Different orientations of 162 the molecule have been tested. The adsorption energy $E_{\rm ads}$ is 163 calculated as the energy difference between the energy of the 164 adsorption complex and the sum of the gas-phase molecule and 165 the bare slab. In our convention, if the adsorption stabilizes the 166 system, then $E_{\rm ads}$ <0. Thus, the more negative the $E_{\rm ads}$, the more 167 stable is the system.

Adsorption Systems. Multiple possibilities of dopamine 169 adsorption were considered, and the most stable ones are 170 depicted in Figure 1. Table 1 shows the adsorption energies for 171 ft each surface orientation. The molecule dissociates by its OH 172 bonds and adsorbs on two under-coordinated Ti sites forming 173 two Ti_{surf}O and two O_{surf}H bonds; this is the bidentate mode. 174 Neither the molecular mode, i.e., without OH dissociation, nor 175 the partially dissociated modes are found to be as stable as the 176 fully deprotonated one. Dopamine stays perpendicular to the 177 surface in all cases. The monodentate mode (one oxygen of the 178 molecule on one Ti site, the other as OH group) and the 179 chelated (two oxygen sites of the molecule on one Ti site) 180

Figure 1. Gas-phase dopamine and most stable adsorption systems obtained for the (001), (100), and (101) anatase terminations.

181 evolve during the optimization to the bidentate one for the 182 (001) termination. This mode is suggested as the most stable 183 one in experimental works, 12 although in ref 12 the authors do 184 not discard the presence of other modes. The adsorption 185 through two oxygen atoms supports theoretical calculations of 186 catechol on anatase TiO_2 by Redfern et al. 30 In ref 15, catechol 187 adsorption on the (101) periodic slabs gives an adsorption 188 energy of -0.94 eV for a thinner slab model (three TiO_2 189 bilayers in ref 15; six TiO_2 bilayers in the present work). Liu et 190 al. 15 report an adsorption energy of -0.70 eV for the catechol 191 bidentate mode at the diluted limit on anatase (101).

As we see from Table 1 and Figure 1, the most favorable 193 adsorption energy is found for the (001) orientation, $E_{\rm ads}$ = 194 -1.86 eV, followed by the (100) with $E_{\rm ads}$ = -1.14 eV. The 195 (101) slab shows $E_{\rm ads}$ = -0.67 eV. These values follow the 196 expected trend of reactivity to molecule adsorption with respect 197 to the bare surface, i.e., the (001) and (100) terminations are 198 more stabilized than the (101) when the molecule adsorbs. 199 This is explained by the lower reactivity of the (101) bare slab, 200 which is known to be the most stable. According to our results, 201 dopamine shows a stronger affinity for (001) and (100) planes. 202 Whereas the order of stability for the bare surfaces decreases as 203 follows: (101) > (001) > (100). The stability of the covered 204 slabs depends on the nature of the adsorbate, and the order is 205 substantially different. 32,33 This is the case for dopamine.

Bader population analysis³⁴ has been carried out for the bidentate adsorption modes of Figure 1, and Bader charges for selected atoms are given in Table 2. It can be observed that the dopamine molecule transfers 0.77 lel (001), 0.81 lel (100), and 0.82 lel (101) to the slab upon adsorption in the bidentate mode becoming positively charged. The transferred electrons come mainly from the oxygen atoms, whose charge decreases

Table 2. Bader Charges for Selected Atoms and Groups of Atoms in lel^a

	(001)	(100)	(101)	gas-phase dopamine
dopamine	+0.77	+0.81	+0.82	0.00
OH groups	-1.20	-1.15	-1.14	-1.66
cycle	1.93	1.89	1.91	1.64
$CH_2CH_2NH_2$	0.04	0.07	0.05	0.02
Ti-O-C	-1.60	-1.68	-1.69	-1.83
slab	-0.77	-0.81	-0.82	
Ti-O-C	+2.60	+2.62	+2.63	
O-H	-1.68	-1.68	-1.69	
$\mathrm{Ti}_{\mathrm{bulk}}$	+2.64	+2.63	+2.65	
O_{bulk}	-1.32	-1.32	-1.33	

^aModels are in Figure 1.

from -1.83 lel in the gas-phase to -1.60/-1.69 lel for the 213 adsorbed systems, and from the aromatic cycle, whose charge 214 passes from +1.64 lel in the gas-phase to $\sim+1.90$ lel; see Table 215 2. The slab becomes thus negatively charged upon adsorption. 216 This extra charge is mainly located on the surface hydroxyl 217 groups, with an oxygen charge of approximately -1.68 lel to be 218 compared with the bulk oxygen charge of -1.32 lel. Also, the 219 surface titanium sites bonded to dopamine exhibit a charge of 220 +2.60/+2.63 lel, which is slightly less positive than the Ti in the 221 bulk charged +2.63/+2.65 lel.

Regarding the dissociation of the dopamine OH groups, the 223 process obeys an acid—base adsorption mechanism³⁵ where the 224 surface oxygen sites would be more basic than the molecule 225 ones, inducing the migration of the H^+ groups to bind to the 226 former. Liu et al. found energetic barriers for catechol 227 dissociation of 0.45 eV (first deprotonation) and 0.40 eV 228 (second deprotonation), which indicate easy deprotonation and 229 interconversion on the (101) termination, supported by 230 scanning tunneling microscopy observations.

Electronic Structure: DOS and Spin Distribution. The 232 dopamine and slab-projected DOS calculated for the most 233 stable systems found for the three anatase terminations are 234 shown in Figure 2. The calculated 13 Cl band gap found for the 235 Cl three slab models is approximately 2 eV, and the experimental 236 value of $^{3.2}$ eV is underestimated in pure DFT methods. It can 237 be observed that for the three dopamine adsorption systems a 238 state is present in the middle of the 13 Cl band gap. This state is 239 localized on the molecule and corresponds to the one observed 240 in cluster models too. 20,21 Interestingly, catechol adsorption on 241 13 Cl 242 Cl molecular and monodentate modes. For lower energies, it is 243 Cl found that the valence band of the slab is mainly formed by 244 Cl oxygen p states, whereas for higher energies, the conduction 245 Cl band is mainly composed of Ti 246 Cl and 246

A comparison of the three terminations shows that in the 247 (001) adsorption system the molecular level is closer to the 248 conduction band than for either the (100) or the (101) slabs. 249 Although the analysis is not quantitative, this might be 250 connected to a better coupling of the molecule with this 251 surface and is consistent with the high adsorption energy found 252 for this system. In the three cases studied, the excited states of 253 the molecule do not lie in the lower part of the conduction 254 band but at higher energy (for instance, in the (001) system 255 dopamine states lie 2 and 4 eV above the Fermi energy). This 256 might be an indication of a direct photoinjection mechanism 257 without the intervention of an intermediate excited state as has 258 been proposed in the literature for catechol. 15 In the direct 259 photoinjection mechanism, the molecular excited states lie 260 within the conduction band, mixed with the host electronic 261 states. In order to check if the electronic structure is influenced 262

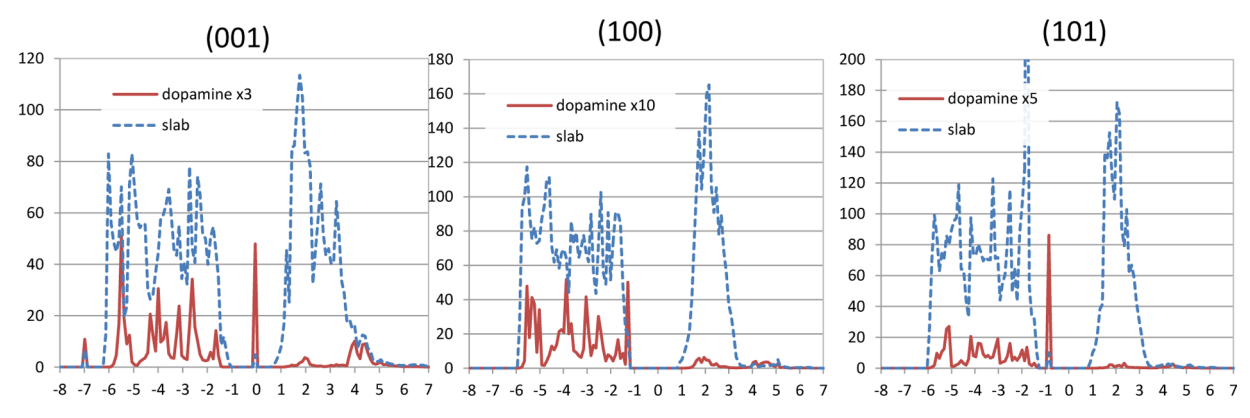


Figure 2. Dopamine and slab-projected DOS for the three terminations of anatase calculated at the PBE level; models are shown in Figure 1. The Fermi level is shifted to the zero energy. y axis, DOS is in arbitrary units; x axis, energy is in eV.

263 by the inherent problems of pure GGA functionals, we have 264 calculated the DOS of the three structures with PBE+U (U-J = 265 4); the plots are displayed in Supporting Information. The 266 main change observed corresponds to a shift to higher energies 267 of the bottom of the conduction band, as expected from the 268 inclusion of the U-J = 4 for Ti 3d levels, and the band gap is 269 therefore increased. The presence of a molecular state in the 270 gap as well as the mixing of molecular excited states with the 271 TiO₂ conduction band is preserved when including the 272 Hubbard correction.

In order to mimic the excitation by a laser field, the triplet the states of the three adsorption systems selected have been calculated. In these excited states, the optimized geometry is kept fixed, and one electron is promoted to the conduction band, keeping the difference between alpha and beta electrons equal to 2. The calculated singlet—triplet energy gap is given in Table 3 for the GGA and GGA+U calculations. The (001) slab

Table 3. Singlet–Triplet Gap Obtained for GGA and GGA +U (U-J = 4 eV) in eV

	GGA	GGA+U
(001)	1.82	1.96
(100)	1.91	2.10
(101)	1.94	2.20

280 model shows the narrowest gap, followed by (100) and (101) 281 models. Also, it can be observed that the GGA+U values are 282 larger than the pure GGA values, as expected from the inclusion 283 of the Hubbard parameter on the Ti 3d states but with same 284 trends with regard to the surface termination.

The visualization of the $N_{\alpha-\beta}$ spin density in the triplet state is shown in Figure 3 for the three systems. In this representation, the isosurface of the $N_{\alpha-\beta}$ spin density is session to the molecule (aromatic ring and oxygen sites bonded to the surface) as well as on a single surface titanium site, as corresponds to the occupation of both the HOMO and LUMO states by one electron each. This picture supports a charge transfer mechanism that would take place from the molecule to the surface resulting in an increase of the transition dipole moment.

Bader population analysis has been carried out for the spin density of the triplet states at the GGA+U level and is summarized in Table 4. It can be seen that upon excitation from the singlet to the triplet state, the contribution of the dopamine fragment is 0.84/0.93, essentially localized at the

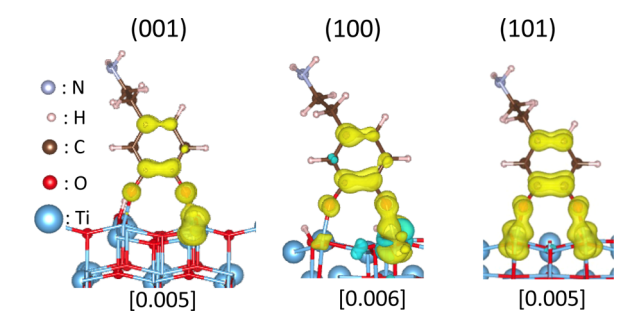


Figure 3. Spin localization in the triplet state for the dopamine adsorbed on the three anatase slabs. The spin isosurfaces are displayed in yellow. In square brackets are the isocontour values in eV/A^3 . The Vesta program³⁷ has been used for visualization.

Table 4. Bader Population Analysis for the Spin Density of GGA+U Triplet States, Computed for Selected Atoms and Groups As in Figure 1

	(001)	(100)	(101)
dopamine	0.87	0.93	0.84
OH groups	0.14/0.21	0.15/0.16	0.16/0.20
cycle	0.51	0.60	0.47
CH ₂ CH ₂ NH ₂	0.01	0.01	0.00
slab	1.12	1.06	1.15
Ti-O-C	0.11/0.84	0.53/0.45	0.13/0.83

aromatic ring (0.47/0.60) and on the oxygen atoms (0.14/3000.21). The slab's contribution accounts for the rest, 1.06/1.12, 3010 essentially localized on the Ti surface sites bonded to the 3020 dopamine. Note that for the model (100), the two Ti sites 3030 bonded to the molecule possess a similar spin density, 0.45/3040.53, whereas for (001) and (101), one titanium site 3050 concentrates the spin, 0.11/0.84 and 0.13/0.83, respectively. 3060 This spin distribution is again consistent with the charge 3070 transfer mechanism responsible for the SERS effect.

CONCLUSIONS

Collecting all of the information above the following statements 310 concerning the dopamine interaction with ${\rm TiO_2}$ surfaces we can 311 draw the following conclusions: (1) Dopamine adsorption is 312 energetically favorable in the three terminations of the bare 313 anatase studied. The molecule deprotonates and binds to two 314 surface titanium sites in a bidentate mode. (2) (001) exhibits a 315 more favorable adsorption energy, -1.82 eV compared to the 316 (100) termination, which is -1.14 eV. The least favorable 317

318 adsorption is found for the (101) terminated slab, -0.67 eV. 319 This indicates clearly a preference of the dopamine molecule 320 for the (001) slab. (3) Upon adsorption, the dopamine 321 molecule forms a charge transfer complex and transfers $\sim 0.7/322$ 0.8 electrons to the anatase surface. Also, the electronic 323 structure displays a state in the TiO_2 band gap that corresponds 324 to the molecule (HOMO), whereas the conduction band 325 corresponds to empty titanium 3d states (LUMO). This picture 326 is consistent with a charge transfer mechanism from the 327 molecule to the semiconductor slab. (4) Excitation of the 328 system to a triplet state involves the promotion of an electron 329 from the molecule to the surface titanium sites.

Although the models used consider perfect stoichiometric infinite slabs, they help to understand the mechanisms of adsorption. The electronic structure of dopamine adsorbed on anatase surfaces explains key experimental results about SERS. The charge transfer mechanism suggested in the literature, involving the excitation of electrons from the molecule to the surface, is supported by our results. Further investigations are needed to address the role of the solvent, in particular in the system protonation of the amine group, as well as the presence of system structural (steps and reconstruction) and electronic (titanium reduction) defects in the charge transfer mechanism.

341 ASSOCIATED CONTENT

342 S Supporting Information

343 Optimized structures for dopamine adsorbed on (001), (100), 344 and (101) anatase slabs; atomic Bader charges of the gas-phase 345 molecule and differences between the gas-phase and the 346 adsorbed molecule; and slab and dopamine projected DOS 347 obtained with PBE+U (U-J = 4). This material is available free 348 of charge via the Internet at http://pubs.acs.org.

349 AUTHOR INFORMATION

sso Corresponding Author

351 *Phone: +33 1 44 27 25 05. Fax: +33 1 44 27 41 17. E-mail: 352 calatayu@lct.jussieu.fr.

S Notes

354 The authors declare no competing financial interest.

355 **ACKNOWLEDGMENTS**

356 This work was financially supported by project NSF-ANR 357 (ANR-11-NS04-0001 FRAMOLSENT program). This work 358 was performed using HPC resources from GENCI-CINES/359 IDRIS (Grants 2012-x2012082131, 2013-x2013082131, and 360 2014-x2014082131) and the CCRE-DSI of Université P. M. 361 Curie. Dr. B. Diawara is warmly acknowledged for the 362 Modelview visualization program. We also acknowledge Dr. 363 Enrique Poulain at FAMA, UAM unidad Azcapotzalco, Mexico, 364 for the facilities. D.F.S. acknowledges the Research in Paris 365 program for a postdoctoral grant.

366 REFERENCES

- 367 (1) Chen, X.; Mao, S. S. Titanium Dioxide Nanomaterials: Synthesis, 368 Properties, Modifications, and Applications. *Chem. Rev.* **2007**, *107*, 369 2891–2959.
- 370 (2) Linsebigler, A. L.; Lu, G.; Yates, J. T. Photocatalysis on TiO_2 371 Surfaces: Principles, Mechanisms, and Selected Results. *Chem. Rev.* 372 **1995**, 95, 735–758.
- 373 (3) Finkelstein-Shapiro, D.; Tarakeshwar, P.; Rajh, T.; Mujica, V. 374 Photoinduced Kinetics of Sers in Bioinorganic Hybrid Systems. A Case 375 Study: Dopamine-TiO₂. *J. Phys. Chem. B* **2010**, *114*, 14642–14645.

- (4) Musumeci, A.; Gosztola, D.; Schiller, T.; Dimitrijevic, N. M.; 376 Mujica, V.; Martin, D.; Rajh, T. SERS of Semiconducting Nano- 377 particles (TiO₂ Hybrid Composites). *J. Am. Chem. Soc.* **2009**, *131*, 378 6040–6041.
- (5) Yang, L.; Jiang, X.; Ruan, W.; Zhao, B.; Xu, W.; Lombardi, J. R. 380 Adsorption Study of 4-MBA on TiO₂ Nanoparticles by Surface- 381 Enhanced Raman Spectroscopy. *J. Raman Spectrosc.* **2009**, *40*, 2004— 382 2008.
- (6) Pérez Leon, C.; Kador, L.; Peng, B.; Thelakkat, M. Character- 384 ization of the Adsorption of Ru-Bpy Dyes on Mesoporous TiO₂ Films 385 with UV-Vis, Raman, and FTIR Spectroscopies. *J. Phys. Chem. B* **2006**, 386 110, 8723–8730.
- (7) Quagliano, L. G. Observation of Molecules Adsorbed on III-V 388 Semiconductor Quantum Dots by Surface-Enhanced Raman Scatter- 389 ing. J. Am. Chem. Soc. 2004, 126, 7393–7398.
- (8) Hayashi, S.; Koh, R.; Ichiyama, Y.; Yamamoto, K. Evidence for 391 Surface-Enhanced Raman Scattering on Nonmetallic Surfaces: Copper 392 Phthalocyanine Molecules on Gap Small Particles. *Phys. Rev. Lett.* 393 **1988**, 60, 1085–1088.
- (9) Yamada, H.; Yamamoto, Y.; Tani, N. Surface-Enhanced Raman 395 Scattering (SERS) of Adsorbed Molecules on Smooth Surfaces of 396 Metals and a Metal Oxide. *Chem. Phys. Lett.* **1982**, *86*, 397–400.
- (10) Shoute, L. C. T.; Loppnow, G. R. Excited-State Dynamics of 398 Alizarin-Sensitized TiO₂ Nanoparticles from Resonance Raman 399 Spectroscopy. *J. Chem. Phys.* **2002**, *117*, 842–850.
- (11) Wang, Y.; Hang, K.; Anderson, N. A.; Lian, T. Comparison of 401 Electron Transfer Dynamics in Molecule-to-Nanoparticle and Intramolecular Charge Transfer Complexes. *J. Phys. Chem. B* **2003**, 107, 403 9434–9440.
- (12) Syres, K.; Thomas, A.; Bondino, F.; Malvestuto, M.; Grätzel, M. 405 Dopamine Adsorption on Anatase $TiO_2(101)$: A Photoemission and 406 NEXAFS Spectroscopy Study. *Langmuir* **2010**, 26, 14548–14555.
- (13) Syres, K. L.; Thomas, A. G.; Flavell, W. R.; Spencer, B. F.; 408 Bondino, F.; Malvestuto, M.; Preobrajenski, A.; Grätzel, M. Adsorbate- 409 Induced Modification of Surface Electronic Structure: Pyrocatechol 410 Adsorption on the Anatase TiO₂ (101) and Rutile TiO₂ (110) 411 Surfaces. J. Phys. Chem. C **2012**, 116, 23515–23525.
- (14) Sanchez-de-Armas, R.; San-Miguel, M. A.; Oviedo, J.; Marquez, 413 A.; Sanz, J. F. Electronic Structure and Optical Spectra of Catechol on 414 TiO₂ Nanoparticles from Real Time TD-DFT Simulations. *Phys.* 415 *Chem. Chem. Phys.* **2011**, *13*, 1506–1514.
- (15) Xu, Y.; Chen, W.-K.; Liu, S.-H.; Cao, M.-J.; Li, J.-Q. Interaction 417 of Photoactive Catechol with TiO₂ Anatase (101) Surface: A Periodic 418 Density Functional Theory Study. *Chem. Phys.* **2007**, 331, 275–282. 419
- (16) Nawrocka, A.; Zdyb, A.; Krawczyk, S. Stark Spectroscopy of 420 Charge-Transfer Transitions in Catechol-Sensitized TiO₂ Nano- 421 particles. *Chem. Phys. Lett.* **2009**, 475, 272–276.
- (17) Liu, Y.; Dadap, J. I.; Zimdars, D.; Eisenthal, K. B. Study of 423 Interfacial Charge-Transfer Complex on TiO₂ Particles in Aqueous 424 Suspension by Second-Harmonic Generation. *J. Phys. Chem. B* **1999**, 425 103, 2480–2486.
- (18) Liu, L.-M.; Li, S.-C.; Cheng, H.; Diebold, U.; Selloni, A. Growth 427 and Organization of an Organic Molecular Monolayer on TiO₂: 428 Catechol on Anatase (101). *J. Am. Chem. Soc.* **2011**, 133, 7816–7823. 429 (19) Li, S.-C.; Losovyj, Y.; Diebold, U. Adsorption-Site-Dependent 430 Electronic Structure of Catechol on the Anatase TiO₂(101) Surface. 431 *Langmuir* **2011**, 27, 8600–8604.
- (20) Tarakeshwar, P.; Finkelstein-Shapiro, D.; Hurst, S. J.; Rajh, T.; 433 Mujica, V. Surface-Enhanced Raman Scattering on Semiconducting 434 Oxide Nanoparticles: Oxide Nature, Size, Solvent, and pH Effects. J. 435 Phys. Chem. C 2011, 115, 8994–9004.
- (21) Tarakeshwar, P.; Finkelstein-Shapiro, D.; Rajh, T.; Mujica, V. 437 Quantum Confinement Effects on the Surface Enhanced Raman 438 Spectra of Hybrid Systems Molecule-TiO₂ Nanoparticles. *Int. J.* 439 *Quantum Chem.* **2011**, *111*, 1659–1670.
- (22) Vega-Arroyo, M.; LeBreton, P. R.; Rajh, T.; Zapol, P.; Curtiss, L. 441 A. Density Functional Study of the TiO₂-Dopamine Complex. *Chem.* 442 *Phys. Lett.* **2005**, 406, 306–311.

- (23) Tarakeshwar, P.; Palma, J. L.; Finkelstein-Shapiro, D.; Keller, A.;
- 445 Urdaneta, I.; Calatayud, M.; Atabek, O.; Mujica, V. SERS as a Probe of
- 446 Charge-Transfer Pathways in Hybrid Dye/Molecule-Metal Oxide Complexes. J. Phys. Chem. C 2014, 118, 3774-3782.
- (24) Urdaneta, I.; Pilme, J.; Keller, A.; Atabek, O.; Tarakeshwar, P.;
- 449 Mujica, V.; Calatayud, M. Probing Raman Enhancement in a
- 450 Dopamine-Ti₂O₄ Hybrid Using Stretched Molecular Geometries. J.
- 451 Phys. Chem. A 2014, 118, 1196-1202.
- (25) Kresse, G.; Furthmüller, J. Efficient Iterative Schemes for Ab
- 453 Initio Total-Energy Calculations Using a Plane-Wave Basis Set. Phys. 454 Rev. B 1996, 54, 11169-11186.
- (26) Kresse, G.; Hafner, J. Ab Initio Molecular Dynamics for Open-455 456 Shell Transition Metals. Phys. Rev. B 1993, 48, 13115-13118.
- (27) Perdew, J. P.; Burke, K.; Ernzerhof, M. Generalized Gradient 457
- 458 Approximation Made Simple. Phys. Rev. Lett. 1996, 77, 3865-3868.
- (28) Blochl, P. E. Projector Augmented-Wave Method. Phys. Rev. B 460 **1994**, 50, 17953-17979.
- (29) Kresse, G.; Joubert, D. From Ultrasoft Pseudopotentials to the 461 462 Projector Augmented-Wave Method. Phys. Rev. B 1999, 59, 1758-463 1775
- (30) Redfern, P. C.; Zapol, P.; Curtiss, L. A.; Rajh, T.; Thurnauer, M.
- 465 C. Computational Studies of Catechol and Water Interactions with
- 466 Titanium Oxide Nanoparticles. J. Phys. Chem. B 2003, 107, 11419-467 11427.
- (31) Beltran, A.; Sambrano, J. R.; Calatayud, M.; Sensato, F. R.; 469 Andrés, J. Static Simulation of Bulk and Selected Surfaces of Anatase
- 470 TiO₂. Surf. Sci. 2001, 490, 116-124.
- (32) Barnard, A. S.; Curtiss, L. A. Prediction of TiO₂ Nanoparticle
- 472 Phase and Shape Transitions Controlled by Surface Chemistry. Nano 473 Lett. 2005, 5, 1261-1266.
- (33) Calatayud, M.; Minot, C. Effect of Relaxation on Structure and
- 475 Reactivity of Anatase (100) and (001) Surfaces. Surf. Sci. 2004, 552,
- 476 169-179. (34) Henkelman, G.; Arnaldsson, A.; Jonsson, H. A Fast and Robust 477
- 478 Algorithm for Bader Decomposition of Charge Density. Comput.
- 479 Mater. Sci. 2006, 36, 354-360.
- (35) Calatayud, M.; Markovits, A.; Menetrey, M.; Mguig, B.; Minot,
- 481 C. Adsorption on Perfect and Reduced Surfaces of Metal Oxides.
- 482 Catal. Today 2003, 85, 125-143.
- (36) Di Valentin, C.; Fittipaldi, D. Hole Scavenging by Organic
- 484 Adsorbates on the TiO₂ Surface: A DFT Model Study. J. Phys. Chem.
- 485 Lett. 2013, 4, 1901-1906.
- 486 (37) Momma, K.; Izumi, F. Vesta: A Three-Dimensional Visual-
- 487 ization System for Electronic and Structural Analysis. J. Appl. 488 Crystallogr. 2008, 41, 653-658.